

## Phase separation and insulator-metal behaviour in highly Ba<sup>2+</sup>-doped La<sub>1-x</sub>Ba<sub>x</sub>MnO<sub>3</sub> compounds

This article has been downloaded from IOPscience. Please scroll down to see the full text article.

2002 J. Phys.: Condens. Matter 14 173

(<http://iopscience.iop.org/0953-8984/14/2/305>)

View [the table of contents for this issue](#), or go to the [journal homepage](#) for more

Download details:

IP Address: 171.66.16.238

The article was downloaded on 17/05/2010 at 04:43

Please note that [terms and conditions apply](#).

## Phase separation and insulator–metal behaviour in highly Ba<sup>2+</sup>-doped La<sub>1-x</sub>Ba<sub>x</sub>MnO<sub>3</sub> compounds

S L Yuan, C S Xiong, Z Y Li, Z C Xia, G Q Zhang, G Peng, F Tu,  
Y P Yang, J Liu, L Liu and Y H Xiong

Institute of Materials Physics and Department of Physics, Huazhong University of Science and Technology, Wuhan 430074, People's Republic of China

Received 23 August 2001, in final form 11 October 2001

Published 13 December 2001

Online at [stacks.iop.org/JPhysCM/14/173](http://stacks.iop.org/JPhysCM/14/173)

### Abstract

Investigations of structural and transport features of La<sub>1-x</sub>Ba<sub>x</sub>MnO<sub>3</sub> with  $x = 1/3$  and  $2/3$  are performed. The  $x = 2/3$  sample is shown to be phase separated into a mixture of La<sub>2/3</sub>Ba<sub>1/3</sub>MnO<sub>3</sub> and BaMnO<sub>3</sub> with the same volume fractions, ~50%. In this two-phase system, La<sub>2/3</sub>Ba<sub>1/3</sub>MnO<sub>3</sub> regions are connected in a percolative manner, so the electrical transport is dominated by flow along these percolative paths. Using the recently proposed random resistor network based on electronic phase separation between ferromagnetic metallic and paramagnetic insulating domains, we show that the model can yield results in quantitative agreement with the resistance versus temperature dependence measured for the  $x = 1/3$  and  $2/3$  samples by using the metallic number density as a fitting parameter. This approach suggests a simple quantitative picture that can be used to explain the insulator–metal behaviour in La<sub>1-x</sub>Ba<sub>x</sub>MnO<sub>3</sub> with higher  $x$ .

Doped manganese oxides of the form R<sub>1-x</sub>A<sub>x</sub>MnO<sub>3</sub> (R is a rare-earth ion and A is a divalent ion such as a Ca, Sr, Ba, or Pb ion) have stimulated considerable scientific and technological interest because of their exotic magnetic and electronic properties [1]<sup>1</sup>. Most notable of these properties are the insulator–metal (I–M) behaviour and the colossal magnetoresistance (CMR). Recent studies suggest that these properties tend to be related to intrinsic inhomogeneities due to the presence of strong tendencies toward phase separation (PS) [2]<sup>2</sup>, typically including (1) electronic PS between two different phases that leads to nanometre-scale coexisting clusters and (2) disorder-induced PS that can induce up to micrometre-scale coexisting clusters driven by disorder near the first-order I–M transitions. Experiments on La<sub>0.7</sub>Ca<sub>0.3</sub>MnO<sub>3</sub> near  $T_C$  have indeed indicated the existence of nanometre-scale ferromagnetic metallic (FMM) domains within the paramagnetic insulating (PMI) matrix [3, 4]. Experiments on La<sub>5/8-y</sub>Pr<sub>y</sub>Ca<sub>3/8</sub>MnO<sub>3</sub>, on the other hand, showed the coexistence of micrometre-scale FMM and charge-ordered insulating (COI) domains at low temperatures [5].

<sup>1</sup> For a review of the manganites, see [1].

<sup>2</sup> For a review of phase separation, see [2].

Based on the PS between metallic and insulating domains, two phenomenological approaches to the resistivity of manganites have been proposed by Mayr *et al* [6] and Yuan *et al* [7]. In the approach proposed by Mayr *et al* [6], the authors used the Monte Carlo method to mimic the complicated fractal-like structure in which metallic filaments with resistance  $R_M^{\text{per}}$  are connected in parallel with insulating portions with resistance  $R_I$ . To yield results in agreement with experiments on manganites, the following assumptions are made in their approach: (i)  $R_M^{\text{per}} \ll R_I$  at low temperatures; (ii)  $R_M^{\text{per}} \sim R_I$  at intermediate temperatures; and (iii)  $R_M^{\text{per}} \gg R_I$  at high temperatures. This approach is shown to be appropriate for describing the electrical transport in those manganites, like  $\text{La}_{5/8-y}\text{Pr}_y\text{Ca}_{3/8}\text{MnO}_3$ , in which giant FMM and COI domains coexist. In contrast to this, the approach proposed by Yuan *et al* [7] is based on the existence of FMM domains within the PMI matrix, and assumes that FMM particles (with number density  $p$  which is a function of temperature and magnetic field) and PMI particles randomly occupy the nodes of a network lattice which is realized through the Monte Carlo method. Using  $p(T, H)$  as only fitting parameter whose behaviour is similar to the experimental curve of magnetization, it is found that this approach can yield results in quantitative agreement with experiments on  $\text{R}_{2/3}\text{A}_{1/3}\text{MnO}_3$  (for instance,  $(\text{La}_{0.8}\text{Y}_{0.2})_{2/3}\text{Ca}_{1/3}\text{MnO}_3$  ( $T_C \sim 87$  K),  $\text{La}_{2/3}\text{Ca}_{1/3}\text{MnO}_3$  ( $T_C \sim 250$  K) [7] and  $\text{La}_{2/3}\text{Ba}_{1/3}\text{MnO}_3$  ( $T_C \sim 335$  K) (the present work)). These compounds have tolerance factors ranging between 0.91 and 0.95 and hence cover the whole range in which only PMI and FMM regions are present in the phase diagram [8] of temperature versus tolerance factor developed for  $\text{R}_{1-x}\text{A}_x\text{MnO}_3$  ( $x \sim 0.3$ ).

In addition to the intrinsic PS mentioned above, it is also likely that some manganese perovskites will undergo a different PS into a mixture of two phases with different crystalline structures, which is normally accomplished through the atomic diffusion due to the chemically driven inhomogeneity. This is a conventional structural phase separation (SPS) and is not intrinsic to manganites. Because it is not intrinsic to manganites, the SPS as a physical problem has been less studied for manganites. However, the occurrence of the SPS strongly affects the physical properties of manganites; therefore, it is also important for the correct understanding of manganese physics. In this respect,  $\text{La}_{1-x}\text{Ba}_x\text{MnO}_3$  may provide a prototypical example. Earlier measurements of x-ray diffraction (XRD) by and the micro-Raman spectrum of  $\text{La}_{1-x}\text{Ba}_x\text{MnO}_3$  revealed that the perovskite structure is stable for  $x \leq 0.35$  while the SPS occurs for  $x > 0.35$  [9–11]. This is different from the case for  $\text{La}_{1-x}\text{Ca}_x\text{MnO}_3$ , in which the perovskite structure is stable for the whole composition range [13]. This difference leads to different observations of physical properties in the two systems. In particular,  $\text{La}_{1-x}\text{Ba}_x\text{MnO}_3$  is ferromagnetic at low temperatures and shows I–M behaviour even for  $x$  as high as 0.75 [11, 12]. The purpose of the present work is to provide a possible scenario for the interpretation of the electrical transport observed in  $\text{La}_{1-x}\text{Ba}_x\text{MnO}_3$  with higher  $x$ , based on our analysis of crystalline structure, transport behaviour and Monte Carlo simulation of the resistance versus temperature dependence using the phenomenological model [7] proposed recently.

Two samples with typical compositions,  $\text{La}_{2/3}\text{Ba}_{1/3}\text{MnO}_3$  and  $\text{La}_{1/3}\text{Ba}_{2/3}\text{MnO}_3$ , were used in the present study; these were fabricated by the conventional solid-state reaction method. Stoichiometric amounts of the starting materials  $\text{La}_2\text{O}_3$ ,  $\text{BaCO}_3$  and  $\text{MnCO}_3$  were mixed thoroughly and calcined at  $\sim 1000$  °C for 24 h. The powder thus obtained was ground, pelletized and sintered at  $\sim 1300$  °C for 24 h, with one intermediate grinding, and then furnace cooled to room temperature.

The structural characterization was done by means of XRD at room temperature with Cu  $K\alpha$  radiation. Shown in figure 1 are XRD patterns for both samples. The  $x = 1/3$  sample, as indicated in figure 1(a), crystallizes in a single phase, showing the characteristic peaks of the perovskite structure similar to those previously reported [10] for similar compositions.

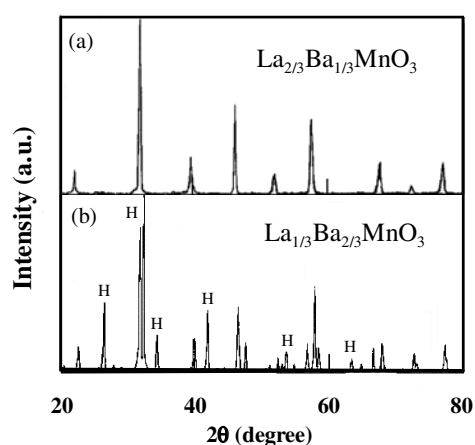


**Figure 1.** The XRD pattern measured for La<sub>1-x</sub>Ba<sub>x</sub>MnO<sub>3</sub> with  $x = 1/3$  (a) and  $2/3$  (b). The XRD peaks from the hexagonal phase are marked by 'H'.

For the  $x = 2/3$  sample, as shown in figure 1(b), the XRD peaks are composed of diffraction peaks from the perovskite structure and some additional XRD peaks marked by H. According to earlier studies on similar compounds [9, 10], these additional XRD peaks are due to the presence of hexagonal BaMnO<sub>3</sub>. This implies that La<sub>1/3</sub>Ba<sub>2/3</sub>MnO<sub>3</sub> is phase separated into a mixture of La<sub>2/3</sub>Ba<sub>1/3</sub>MnO<sub>3</sub> perovskite and BaMnO<sub>3</sub> hexagonal phase. For the sake of discussion, we consider the more general case in which La<sub>1-x</sub>Ba<sub>x</sub>MnO<sub>3</sub> with  $x \geq 1/3$  is separated into La<sub>2/3</sub>Ba<sub>1/3</sub>MnO<sub>3</sub> and BaMnO<sub>3</sub>, i.e., La<sub>1-x</sub>Ba<sub>x</sub>MnO<sub>3</sub>  $\rightarrow$   $(1-y)$ La<sub>2/3</sub>Ba<sub>1/3</sub>MnO<sub>3</sub> +  $y$ BaMnO<sub>3</sub>, where  $y = \frac{1}{2}(3x - 1)$  and  $1 - y = \frac{3}{2}(1 - x)$  are the volume fractions of BaMnO<sub>3</sub> and La<sub>2/3</sub>Ba<sub>1/3</sub>MnO<sub>3</sub>, respectively. Systematic investigations on La<sub>1-x</sub>Ba<sub>x</sub>MnO<sub>3</sub> show that SPS occurs as  $x$  exceeds  $1/3$  and the volume fraction of the hexagonal phase increases with further increasing  $x$  [9, 10, 12]. For the present special composition (i.e.,  $x = 2/3$ ), the two phases have close volume fractions,  $\sim 50\%$ . This can be confirmed from the XRD patterns, in which the relative intensities of the XRD peak near  $2\theta = 30^\circ$  for the two phases are close.

The electrical transport is studied experimentally by measuring resistivity as a function of temperature by means of the standard four-probe method. The results are shown in figure 2 for both samples. The  $x = 1/3$  sample shows thermally activated insulating-like behaviour at high temperatures, with resistivity rising on cooling. After the resistivity passes through a maximum at  $T_p \sim 330$  K, further cooling brings about a sharp reduction in it, indicating metallic behaviour. For the  $x = 2/3$  sample, we also observe the transition to a metallic state; however, the transition becomes smooth and moves towards a lower-temperature region as compared with the  $x = 1/3$  sample. We also note that, compared with the  $x = 1/3$  sample, both the peak value and the low-temperature resistivity are clearly increased for the  $x = 2/3$  sample. Systematic investigations on La<sub>1-x</sub>Ba<sub>x</sub>MnO<sub>3</sub> indicate that the behaviour observed for the  $x = 2/3$  sample seems to be a property common to samples with  $x$  between 0.5 and 0.75 [12]. As  $x$  exceeds 0.75, the sample shows typical insulating behaviour over the whole temperature range. It is interesting to note that, except for different magnitudes of resistivity, the temperature dependences of the resistivity are almost identical for samples with  $x$  between 0.5 and 0.75 [12].

On the basis of the SPS found from the XRD, a possible scenario for the interpretation of the experimental observations mentioned above is as follows. BaMnO<sub>3</sub> is insulating over the whole temperature range studied. La<sub>2/3</sub>Ba<sub>1/3</sub>MnO<sub>3</sub>, on the other hand, is PMI above  $T_C$ ,

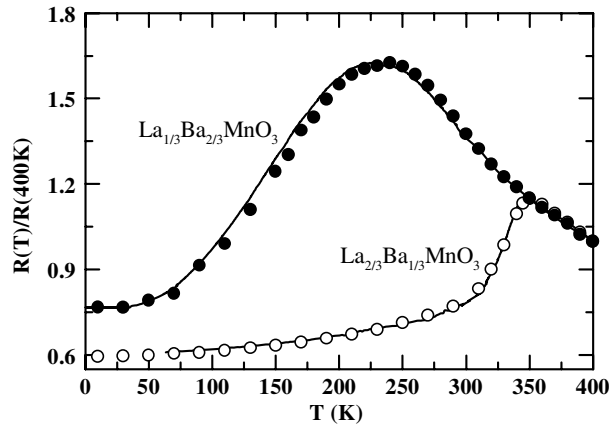


**Figure 2.** Temperature dependences of the resistance for  $\text{La}_{1-x}\text{Ba}_x\text{MnO}_3$  with  $x = 1/3$  and  $2/3$ , where the resistance is normalized by the resistance value at  $T = 400$  K. The solid curves are experimental curves and the symbols represent simulated data (see the text).

but its room temperature resistivity ( $\sim 10^{-2} \Omega \text{ cm}$ ) is larger at least by four orders than that of  $\text{BaMnO}_3$  [12]. It is therefore reasonable to argue that  $\text{La}_{1/3}\text{Ba}_{2/3}\text{MnO}_3$  is a two-phase system consisting of a conducting phase,  $\text{La}_{2/3}\text{Ba}_{1/3}\text{MnO}_3$ , and an insulating phase,  $\text{BaMnO}_3$ , having the same volume fraction,  $\sim 50\%$ . Since the conductor fraction is larger than the percolation threshold ( $\sim 30\%$  for three dimensions [14]), we expect the conductor regions to be connected in a percolative manner, which is schematically illustrated by the dark area in figure 3(a). The total sample resistance can then be obtained by considering a simple system of two parallel resistances, as indicated in figure 3(b), where  $R^{\text{per}}$  and  $R^I$  are the resistances of the percolative paths (dark area in figure 3(a)) from the conducting phase  $\text{La}_{2/3}\text{Ba}_{1/3}\text{MnO}_3$  and of the paths (white area in figure 3(a)) from the insulating phase  $\text{BaMnO}_3$ , respectively. Since  $R^I \gg R^{\text{per}}$ , current can flow actually only along the percolative paths. This means that the transport behaviour in  $\text{La}_{1/3}\text{Ba}_{2/3}\text{MnO}_3$  is actually dominated by  $\text{La}_{2/3}\text{Ba}_{1/3}\text{MnO}_3$ . This suggests a simple qualitative picture that can be used to visualize why the resistivity in this compound has the peculiar shape it has. Similar reasoning is also appropriate for the other samples with higher  $x$ —for instance,  $x = 0.75$ . For this composition, the volume fraction of conductors is simply estimated to be  $\sim 37.5\%$ , which is still larger than the percolation threshold, so its transport behaviour is dominated by the percolative  $\text{La}_{2/3}\text{Ba}_{1/3}\text{MnO}_3$  paths. This suggests a simple interpretation of previous experimental observations [12] that indicate resistance dependences on temperature that are almost the same for samples with  $x = 0.63$  and  $0.75$ . Our interpretation can be also supported by the following experimental fact: the disappearance of I–M behaviour in  $\text{La}_{1-x}\text{Ba}_x\text{MnO}_3$  as  $x$  exceeds a value which is empirically found to be between  $0.75$  and  $0.88$  [12]. In the present case, using  $30\%$  (the percolation threshold) as the value of the conductor fraction below which the conducting regions are disconnected from each other, we can then infer that as  $x \geq 0.8$ , the sample becomes insulating over the whole temperature range. This is in good agreement with previous experiments [12].

From the above discussion, we know that the transport in  $\text{La}_{1/3}\text{Ba}_{2/3}\text{MnO}_3$  is actually dominated by  $\text{La}_{2/3}\text{Ba}_{1/3}\text{MnO}_3$  conductors which are connected in a percolative manner. As shown in figure 2, however, the I–M behaviour in the  $x = 2/3$  sample is clearly different from that of the  $x = 1/3$  sample, suggesting that the effect caused by the presence of the insulating  $\text{BaMnO}_3$  phase in  $\text{La}_{1/3}\text{Ba}_{2/3}\text{MnO}_3$  still needs to be considered. This can be understood from the following approach to the temperature dependences of the resistance measured for the

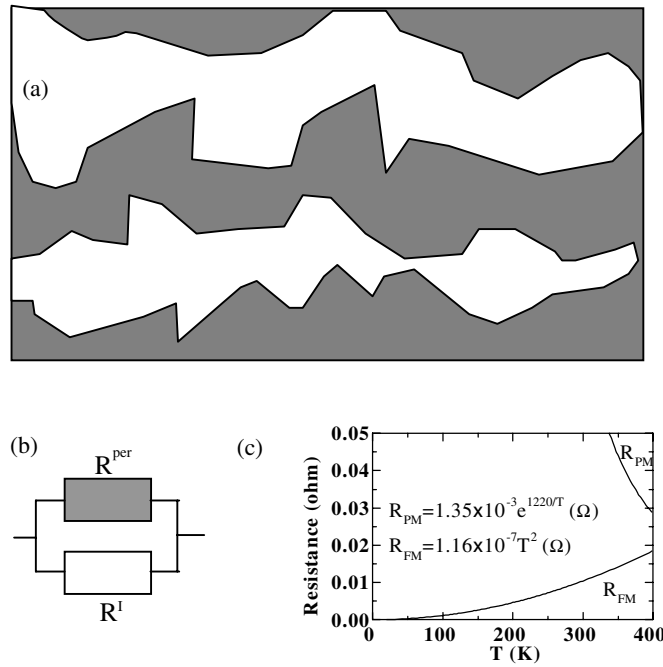


**Figure 3.** (a) A schematic illustration of the SPS between conducting  $\text{La}_{2/3}\text{Ba}_{1/3}\text{MnO}_3$  regions (dark area) and insulating  $\text{BaMnO}_3$  regions (white area). (b) The two-resistance model for the situation indicated in (a). (c) Temperature dependences of  $R_{\text{PM}}$  and  $R_{\text{FM}}$  used in the simulation (see the text).

two samples using the recently proposed random-resistor-network model [7] based on the electronic PS between PMI and FMM domains.

The physical basis and main assumptions for the random-resistor-network model proposed in [7] are summarized here.

- (1) The sample is phase separated near  $T_C$  into a mixture of FMM and PMI domains.
- (2) These domains are modelled as particles that randomly occupy the nodes of a network lattice.
- (3) The kind of particle residing at the  $i$ th node depends on the value of a computer-generated random number. If this number is smaller than the chosen  $p$ -value, this node is assigned a FMM particle; otherwise it is assigned a PMI particle. Here  $p$  is the number density of FMM particles.
- (4) Current is conducted through a ‘bond resistance’  $R_{ij}$  between two adjacent nodes. As two adjacent nodes are occupied by FMM (or PMI) particles,  $R_{ij}$  is determined as  $R_{ij} = R_{\text{FM}}$  (or  $R_{\text{PM}}$ ), where  $R_{\text{FM}}$  ( $R_{\text{PM}}$ ) is the resistance of the individual FMM (PMI) particles; while as two adjacent nodes are occupied by particles of different kinds,  $R_{ij}$  is determined by  $R_{ij}^{-1} = R_{\text{PM}}^{-1} + R_{\text{FM}}^{-1}$ .

Through this process, the random resistor network is constructed and the sample resistance is then obtained by solving the Kirchhoff equations using a simple iterative procedure.

Three quantities,  $R_{\text{FM}}$ ,  $R_{\text{PM}}$  and  $p$ , are involved in the above-mentioned model. For a pure  $\text{La}_{2/3}\text{Ba}_{1/3}\text{MnO}_3$  sample,  $R_{\text{PM}}$  and  $R_{\text{FM}}$  can be directly extracted from the resistance versus temperature dependences measured at  $T \gg T_C$  and  $T \ll T_C$ , respectively. The thus-obtained

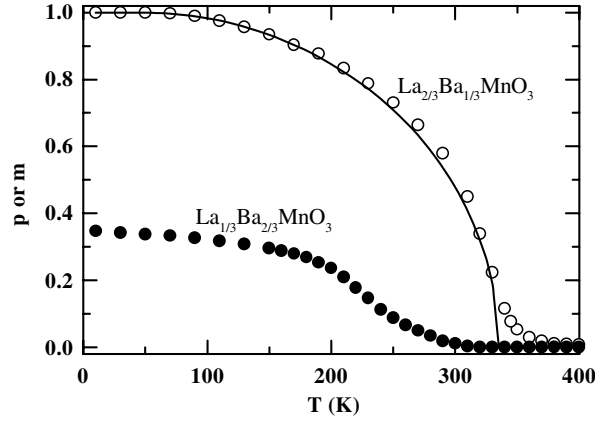


**Figure 4.** Temperature dependences of the number density of FMM particles,  $p(T)$ , used in the simulation of  $R(T)$  for  $\text{La}_{1-x}\text{Ba}_x\text{MnO}_3$  with  $x = 1/3$  (open circles) and  $2/3$  (solid circles). The reduced magnetization  $m$  (solid curve) as a function of temperature is also plotted for comparison.

$R_{PM}$  and  $R_{FM}$ , as functions of temperature, are plotted in figure 3(c). Because  $p$  is the number density of FMM particles, it should be proportional to the volume fraction of FM phase and hence to the spontaneous magnetization  $M_s$ . It is therefore reasonable to consider  $p(T)$  as  $p(T) = M_s(T)/M^{\text{sat}}$ , where  $M^{\text{sat}}$  is the saturation magnetization corresponding to the full ordered moment of Mn ions. Assuming the sample to be of high quality, it is then expected that the sample will show robust FM behaviour at low temperatures, implying that  $M_s(T) \rightarrow M^{\text{sat}}$  or  $p(T) \rightarrow 100\%$  as  $T \rightarrow 0$  K. Near or above  $T_C$ , as revealed in experiments [15], there is a tail on the magnetization versus temperature curve which can extend up a temperature much higher than  $T_C$ . In view of this fact, we have actually assumed  $p(T)$  to be as indicated by the open circles in figure 4; it is used as a fitting parameter for the simulation of the  $R$  versus  $T$  dependence for the pure  $\text{La}_{2/3}\text{Ba}_{1/3}\text{MnO}_3$  sample. For comparison, in figure 4 we also plot the reduced magnetization  $m(T)$  (solid curve) calculated from the mean-field self-consistency equation [16]

$$m = B_J \left( \frac{3J}{J+1} \frac{m}{t} \right) \quad (1)$$

with  $J = 1.83$  and  $T_C = 335$  K, where  $B_J$  is the Brillouin function and  $t = T/T_C$  is the reduced temperature. It can be found that, except for the temperature range near  $T_C$ , no difference exists between the two sets of curves,  $p(T)$  and  $m(T)$ . Using the thus-obtained  $R_{PM}$ ,  $R_{FM}$  and  $p$ , we can obtain a simulation curve for the resistance versus temperature dependence. The simulated results (open circles) as indicated in figure 2 show excellent agreement with experimental data (solid curve) measured for  $\text{La}_{2/3}\text{Ba}_{1/3}\text{MnO}_3$ .

A similar simulation can also be performed for the resistance versus temperature dependence measured for  $\text{La}_{1/3}\text{Ba}_{2/3}\text{MnO}_3$ . The results are displayed by solid circles in figure 2, together with the corresponding experimental data (solid curve); these show excellent agreement. In this simulation, we keep both  $R_{PM}$  and  $R_{FM}$  the same as for pure  $\text{La}_{2/3}\text{Ba}_{1/3}\text{MnO}_3$ , but use  $p$ -values (as indicated by solid circles in figure 4) as fitting parameters to yield results in agreement with experimental data. As discussed above, the transport in  $\text{La}_{1/3}\text{Ba}_{2/3}\text{MnO}_3$  is along the percolative  $\text{La}_{2/3}\text{Ba}_{1/3}\text{MnO}_3$  paths. Therefore, it is reasonable for  $R_{PM}$  and  $R_{FM}$  to be the same for the two samples. One notes that for  $\text{La}_{1/3}\text{Ba}_{2/3}\text{MnO}_3$ , as compared with  $\text{La}_{2/3}\text{Ba}_{1/3}\text{MnO}_3$ ,  $p(T)$  is substantially decreased over the whole temperature

range below  $T_C$  and the maximum value of  $p$  is only  $\sim 0.35$ . This can be understood if one notes the following two facts.

- (1) As discussed above, La<sub>1/3</sub>Ba<sub>2/3</sub>MnO<sub>3</sub> contains  $\sim 50\%$  La<sub>2/3</sub>Ba<sub>1/3</sub>MnO<sub>3</sub>; therefore, the maximum value of  $p$  is only 0.5 even assuming that all Mn spins in this 50% La<sub>2/3</sub>Ba<sub>1/3</sub>MnO<sub>3</sub> are ferromagnetically ordered.
- (2) The presence of BaMnO<sub>3</sub> phase would affect the FM alignment of Mn spins in La<sub>2/3</sub>Ba<sub>1/3</sub>MnO<sub>3</sub>, thus causing further decrease in  $p$ .

In summary, we have investigated both the structural and electrical transport features of La<sub>1-x</sub>Ba<sub>x</sub>MnO<sub>3</sub> with  $x = 1/3$  and  $2/3$ . On the basis of our approach, we propose the possibility of the existence of two kinds of phase separation in La<sub>1-x</sub>Ba<sub>x</sub>MnO<sub>3</sub> with higher  $x$ . One is between conducting La<sub>2/3</sub>Ba<sub>1/3</sub>MnO<sub>3</sub> and insulating BaMnO<sub>3</sub> regions; this is a normal SPS and is not intrinsic in nature. As the volume fraction of conducting La<sub>2/3</sub>Ba<sub>1/3</sub>MnO<sub>3</sub> is above the percolation threshold, the electrical transport in La<sub>1-x</sub>Ba<sub>x</sub>MnO<sub>3</sub> is dominated by the percolative La<sub>2/3</sub>Ba<sub>1/3</sub>MnO<sub>3</sub> paths. The other kind is between FMM and PMI regions; this occurs among the percolative La<sub>2/3</sub>Ba<sub>1/3</sub>MnO<sub>3</sub> paths and is intrinsic to manganites. We therefore believe that La<sub>1-x</sub>Ba<sub>x</sub>MnO<sub>3</sub> is to be regarded as a prototypical compound when studying the PS problem.

### Acknowledgments

This work was supported by the National Science Foundation of China (Grant no 10174022) and the Trans-Century Training Programme Foundation for Talents by the Ministry of Education.

### References

- [1] Coey J M D, Viret M and von Molnar S 1999 *Adv. Phys.* **48** 167  
See also Nagaev E L 2001 *Phys. Rep.* **346** 387
- [2] Dagotto E, Hotta T and Moreo A 2001 *Phys. Rep.* **344** 1
- [3] De Teresa J M *et al* 1997 *Nature* **386** 256
- [4] Uehara M, Mori S and Chen C H 1999 *Nature* **399** 560
- [5] Moreo A, Yunoki S and Dagotto E 1999 *Science* **283** 2034
- [6] Mayr M *et al* 2001 *Phys. Rev. Lett.* **86** 135
- [7] Yuan S L *et al* 2001 *J. Phys.: Condens. Matter* **13** L509  
Yuan S L *et al* 2001 *Appl. Phys. Lett.* **79** 90
- [8] Hwang H Y *et al* 1996 *Phys. Rev. Lett.* **77** 2041
- [9] Roy C and Budhani R C 1998 *Phys. Rev. B* **58** 8174
- [10] Roy C and Budhani R C 1999 *J. Appl. Phys.* **85** 3124
- [11] Budhani R C *et al* 2000 *J. Appl. Phys.* **87** 2490
- [12] Ju H L, Nam Y S, Lee J E and Shin H S 2000 *J. Magn. Magn. Mater.* **219** 1
- [13] Schiffer P *et al* 1995 *Phys. Rev. Lett.* **75** 3336
- [14] Kirkpatrick S 1973 *Rev. Mod. Phys.* **45** 574
- [15] Fontcuberta J *et al* 1996 *Solid State Commun.* **97** 1033
- [16] Kittel C 1986 *Introduction to Solid State Physics* 6th edn (New York: Wiley)